LETTER

doi:10.1038/nature10968

Antarctic ice-sheet loss driven by basal melting of ice shelves

H. D. Pritchard[1], S. R. M. Ligtenberg[2], H. A. Fricker[3], D. G. Vaughan[1], M. R. van den Broeke[2] & L. Padman[4]

Accurate prediction of global sea-level rise requires that we understand the cause of recent, widespread and intensifying[1,2] glacier acceleration along Antarctic ice-sheet coastal margins[3]. Atmospheric and oceanic forcing have the potential to reduce the thickness and extent of floating ice shelves, potentially limiting their ability to buttress the flow of grounded tributary glaciers[4]. Indeed, recent ice-shelf collapse led to retreat and acceleration of several glaciers on the Antarctic Peninsula[5]. But the extent and magnitude of ice-shelf thickness change, the underlying causes of such change, and its link to glacier flow rate are so poorly understood that its future impact on the ice sheets cannot yet be predicted[3]. Here we use satellite laser altimetry and modelling of the surface firn layer to reveal the circum-Antarctic pattern of ice-shelf thinning through increased basal melt. We deduce that this increased melt is the primary control of Antarctic ice-sheet loss, through a reduction in buttressing of the adjacent ice sheet leading to accelerated glacier flow[2]. The highest thinning rates occur where warm water at depth can access thick ice shelves via submarine troughs crossing the continental shelf. Wind forcing could explain the dominant patterns of both basal melting and the surface melting and collapse of Antarctic ice shelves, through ocean upwelling in the Amundsen[6] and Bellingshausen[7] seas, and atmospheric warming on the Antarctic Peninsula[8]. This implies that climate forcing through changing winds influences Antarctic ice-sheet mass balance, and hence global sea level, on annual to decadal timescales.

Over 80% of Antarctica's grounded ice drains through its fringing ice shelves, and glacier flow is sensitive to changes in ice-shelf extent[5] and thickness[4]. Ice-shelf collapse could lead to abrupt and potentially runaway ice-sheet retreat[9]. At their upper surfaces, ice shelves are vulnerable to changes in atmospheric conditions and at their bases they are exposed to heat transported at depth within the Southern Ocean[10]; they lose mass if basal melting or iceberg calving increase, or glacier influx or the surface mass balance (snow accumulation minus ablation) decrease. Basal melt rates vary considerably with thermal forcing: a function of local ocean temperature and ice thickness as the melting point is depressed with depth[11]. The strongest thermal forcing and highest melt rates (over 40 m yr^{-1}) are found near the deep grounding line of Pine Island Glacier, West Antarctica[11], where recent observations have shown enhanced basal melting in response to modest ocean warming and a local feedback between ice-shelf retreat and greater warm-water ingress[10]. Loss of ice-shelf buttressing there[12] has increased the flow rate of grounded ice by 34% from 1996–2006, contributing a sea level rise of 1.2 mm per decade[2]. Ice shelves are thought to be thinning in other locations[13], but the importance of reduced buttressing for ice-sheet dynamics on the continental scale is not known.

Here, we present thickness changes for all of the major Antarctic ice shelves and neighbouring grounded ice for the period 2003–2008. We measure the rate of surface height change ($\Delta h/\Delta t$) by using a time series of repeat-track satellite laser altimetry[1]. The laser altimeter on NASA's ICESat satellite[14] was primarily designed to detect height change on the ice sheets. It has several advantages over satellite radar altimetry (which is traditionally used for this purpose): an orbit that samples all major Antarctic ice shelves; smaller footprints with well-constrained locations and closer along-track spacing; and negligible surface penetration, regardless of season[14].

Our measurements reveal coherent patterns of ice-shelf elevation change rate ($\Delta h/\Delta t$) at the scale of centimetres per year (Fig. 1). A zone of surface lowering on Ross Ice Shelf corresponds to reduced glacier influx following the shutdown of Kamb Ice Stream, where the grounded ice is thickening by up to 0.65 m yr^{-1} (ref. 1). After converting from elevation to thickness change-rate ($\Delta T/\Delta t$) on the ice shelves (Fig. 2), a comparison with results derived from 15 years of radar altimetry[13] shows a broadly similar pattern. However, our measurements increase sampling (from ~12,000 radar altimeter orbit-crossover measurements[13] to ~4.5 million ICESat along-track measurements), extend coverage southwards, improve on the removal of confounding

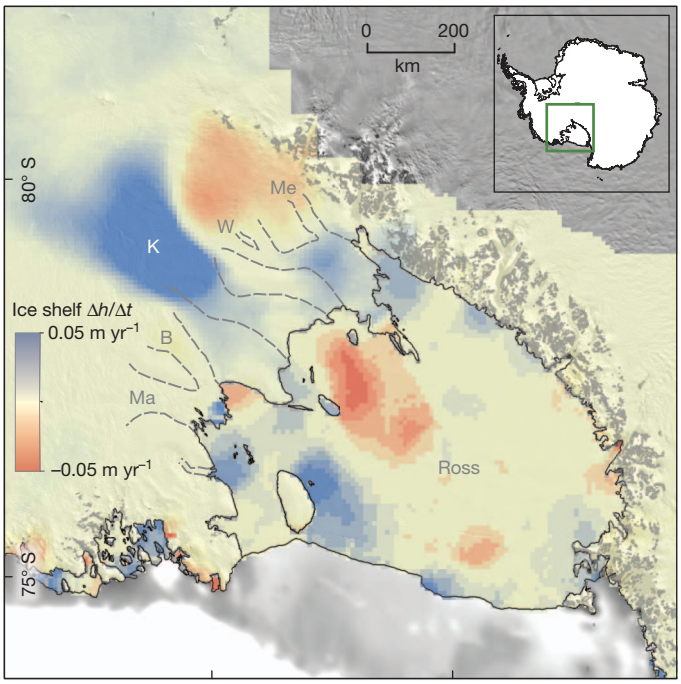

Figure 1 | Surface $\Delta h/\Delta t$ of Ross Ice Shelf, 2003–2008. The colour scale for the grounded ice $\Delta h/\Delta t$ signal is ±30 cm yr^{-1}. The continental shelf is shown in grey, landward of the continental-shelf break[30]. Labels Me, W, K, B and Ma denote the ice streams Mercer, Whillans, Kamb, Bindschadler and MacAyeal. Dashed grey lines show the lateral ice stream margins. Black lines show ice-shelf boundaries (mapped between 1993 and 2003)[31]. The inset shows the location of the figure (green box) overlaid on the outline of Antarctica.

[1]British Antarctic Survey, Natural Environment Research Council, Madingley Road, Cambridge CB3 0ET, UK. [2]Utrecht University, Institute for Marine and Atmospheric Research, 3508 TA Utrecht, The Netherlands. [3]Scripps Institution of Oceanography, University of California San Diego, La Jolla, California 92093, USA. [4]Earth & Space Research, 3350 Southwest Cascade Avenue, Corvallis, Oregon 97333-1536, USA.

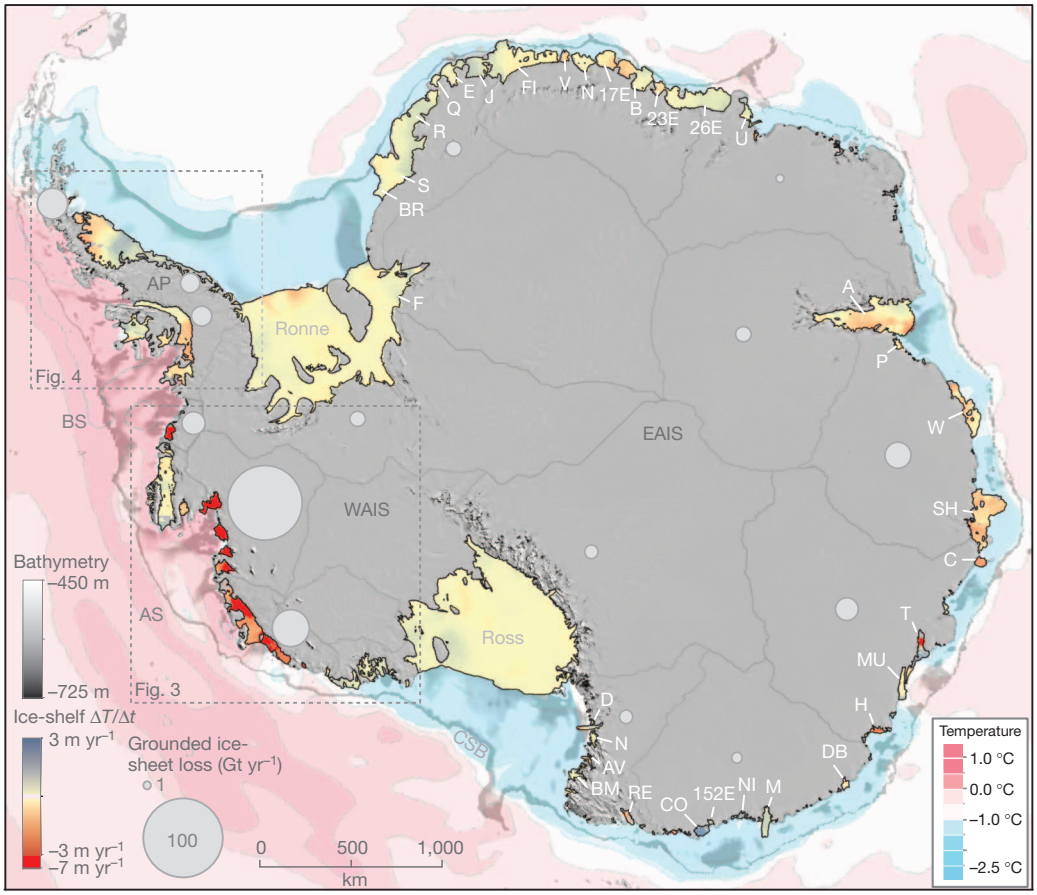

Figure 2 | Antarctic ice-shelf ice-thickness change rate $\Delta T/\Delta t$, 2003–2008. Seaward of the ice shelves, estimated average sea-floor potential temperatures (in °C) from the World Ocean Circulation Experiment Southern Ocean Atlas (pink to blue) are overlaid on continental-shelf bathymetry (in metres)[30] (greyscale, landward of the continental-shelf break, CSB). Grey labels indicate Antarctic Peninsula (AP), West and East Antarctic Ice Sheets (WAIS and EAIS), Bellingshausen Sea (BS), Amundsen Sea (AS) and the Ross and Ronne ice shelves. White labels indicate the ice shelves (clockwise from top) Vigridisen (V), Nivlisen (N), 17 East (17E), Borchgrevinkisen (B), 23 East (23E), 26 East (26E), Unnamed (U), Amery (A), Publications (P), West (W), Shackleton (SH), Conger (C), Totten (T), Moscow University (MU), Holmes (H), Dibble (DB), Mertz (M), Ninnis (NI), 152 East (152E), Cook (CO), Rennick (RE), Borchgrevink-Mariner (BM), Aviator (AV), Nansen (N), Drygalski (D), Filchner (F), Brunt (BR), Stancombe-Wills (S), Riiser-Larsen (R), Quar (Q), Ekstrom (E), Jelbart (J) and Fimble (FI). Grey circles show relative ice losses for ice-sheet drainage basins (outlined in grey) that lost mass between 1992 and 2006 (after ref. 2) (Supplementary Table 1).

signals and separation of surface and basal processes, and show in detail the relationship between thinning of ice shelves and grounded tributary glaciers. These improvements allow us to identify the major cause of grounded Antarctic ice-sheet mass loss.

The distribution of Antarctic ice-shelf thinning ($\Delta T/\Delta t$) is strongly regional (Fig. 2), being most rapid (up to 6.8 m yr^{-1}) along the Amundsen and Bellingshausen Sea coasts. The relatively thick Land, DeVicq, Getz, Dotson, Crosson, Thwaites, Pine Island, Cosgrove and Venable ice shelves thinned during 2003–2008, in marked contrast to the adjacent, thinner Abbott, Nickerson and Sulzberger ice shelves where there was no significant thinning (Fig. 3) (Supplementary Fig. 1, Supplementary Table 1). Firn modelling on the ice shelves (Supplementary Fig. 2) indicates that the firn layer actually thickened throughout this region, mostly through increased accumulation, consistent with ICESat measurements on nearby slow-moving grounded ice (Fig. 3). These neighbouring ice shelves with similar atmospheric forcing but contrasting elevation change signals must therefore be subject to some regional forcing other than local climate. Furthermore, all of the thinning ice shelves maintained their frontal positions or advanced (Supplementary Fig. 3) while simultaneously receiving increased influx from their tributary glaciers[2]. Hence, this regional thinning is not explained by negative surface mass balance, firn compaction, retreating ice-shelf fronts or by reduced glacier influx. We deduce that it is caused by increased basal melt driven by ocean interaction.

Our analysis reveals that there is also evidence of net thinning through enhanced basal melt on the East Antarctic ice shelves Vigridisen, 17E, West, Shackleton, Holmes Glacier, Dibble, Rennick Glacier and the thicker part of Totten. The Nivlisen, Moscow University and 152E ice-shelf surfaces appear to have lowered as a result of firn processes (Fig. 2, Supplementary Figs 4–6, Supplementary Table 1). On the western Antarctic Peninsula, the Stange Ice Shelf and the thicker sections of the George VI Ice Shelf also lowered at a rate greater than the modelled firn-lowering signal in this region, indicating ocean-driven basal melt (Fig. 4, Supplementary Fig. 7). However, the thinning of the retreating Wilkins Ice Shelf during 2003–2008 may combine components of basal melt, surface processes and dynamics (Supplementary Discussion).

An exception to this pattern is the Larsen C ice shelf, where firn processes are an important part of the elevation change signal. Measured $\Delta h/\Delta t$ on the ice shelf increases northwards from −0.06 m yr^{-1} to −0.21 m yr^{-1}, with similar values on adjacent, slow-flowing grounded ice (−0.20 m yr^{-1} in the south to −0.35 m yr^{-1} in the north, on grounded ice at an average 230 m above the ice-shelf altitude; Fig. 4 inset). Our firn modelling independently predicts lowering due to surface processes of −0.10 m yr^{-1} (south) to −0.16 m yr^{-1} (north) for the same period (Fig. 4, Supplementary Table 1). This south–north gradient is echoed in the mapped firn-air content (lesser northwards)[15] and melt days (greater northward), and a temporal trend of +0.5 melt

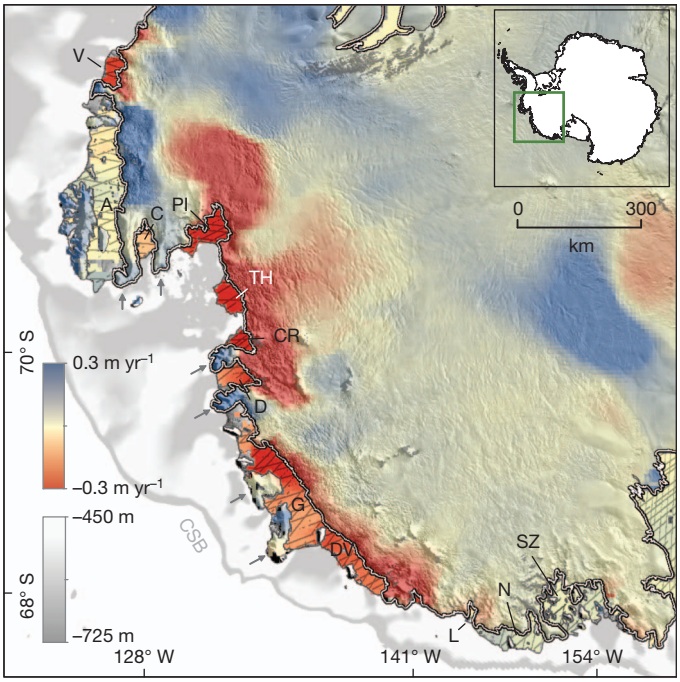

Figure 3 | Surface $\Delta h/\Delta t$ on the ice shelves and grounded ice of the Amundsen/Bellingshausen Sea coasts, 2003–2008. Ice shelves labelled are Venable (V), Abbott (A), Cosgrove (C), Pine Island (PI), Thwaites (TH), Crosson (CR), Dotson (D), Getz (G), De Vicq (DV), Land (L), Nickerson (N) and Sulzberger (SZ). Arrows highlight areas of slow-flowing, grounded ice. Bathymetry[30] landward of the continental-shelf break is in greyscale. Locations of ICESat $\Delta h/\Delta t$ measurements are shown as grey tracks on the ice shelves. The grounding line is in white[31]. The inset shows the location of the figure (green box) overlaid on the outline of Antarctica.

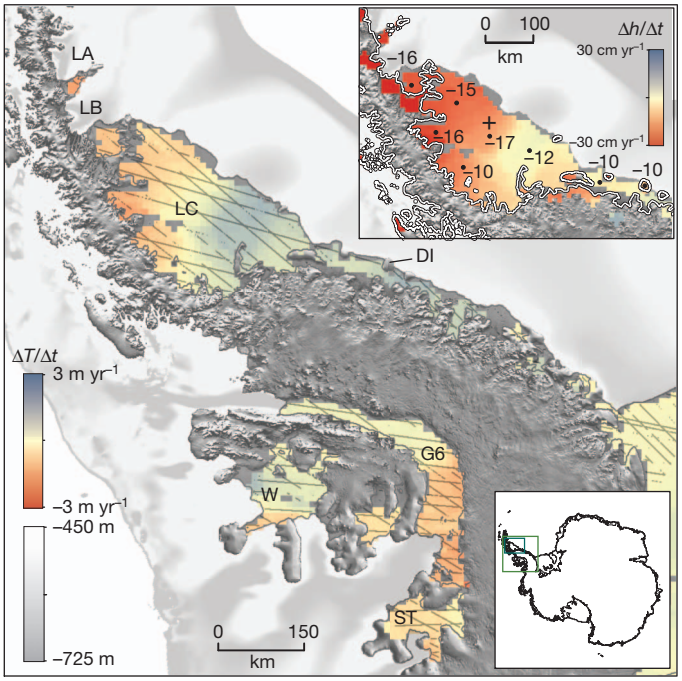

Figure 4 | Ice-shelf $\Delta T/\Delta t$ on the Antarctic Peninsula, 2003–2008. Labelled ice shelves are the former Larsen A and B (LA, LB), Larsen C (LC), George VI (G6), Wilkins (W) and Stange (ST). DI indicates Dolleman Island. Bathymetry[30] landward of the continental-shelf break is in greyscale. Locations of ICESat $\Delta h/\Delta t$ measurements are shown as grey tracks. The upper inset shows $\Delta h/\Delta t$ on Larsen C and adjacent slow-flowing, grounded low-altitude margins, with modelled firn contribution to ice-shelf $\Delta h/\Delta t$ (cm yr^{-1}, at black dots) for 2003–2008. The cross shows the location of the automated weather station used to calibrate the firn model, reducing modelled melt rates by 33%. The grounding line is in white[31]. The lower inset shows the location of the main panel and the inset (bigger and smaller green boxes) overlaid on the outline of Antarctica.

days per year[2] over most of Larsen C from 1979–2009 was reported[16]. We infer that the lowering on the ice shelf and slow-flowing grounded margins is dominated by surface firn processes instead of basal melting, though acceleration of ice-shelf flow in the north may also have contributed to the thinning signal and the modelled firn depth in this area is uncertain (Supplementary Material and Discussion).

Every case of ocean-driven ice-shelf thinning that we identify is linked with previously documented dynamic thinning of grounded, fast-flowing tributary glaciers (Supplementary Table 1)[1,2]. In the absence of significant surface-mass-balance trends (Supplementary Methods 1.2), dynamic thinning accounts for almost all current mass loss from the Antarctic ice sheets and results from glacier acceleration owing to decreased net downstream resistance[1,2]; we attribute this to a reduction in buttressing from the thinning ice shelves[17]. The alternative scenario of dynamic thinning driven by reduced friction at the glacier bed would imply ice-shelf thickening and advance, which is contrary to our observations. A similar attribution of dynamic thinning to ocean-driven melt of marine margins has been made for some Greenland glaciers[18].

Ice-shelf thinning by basal melt implies an increased oceanic heat supply into the sub-ice-shelf cavities. This has been explained by fluctuating incursions of Circumpolar Deep Water (CDW) across the continental shelf of the Amundsen and Bellingshausen seas that sometimes come into contact with the ice-shelf bases, increasing the melt rate[6,7,10]. Originating in the wind-driven Antarctic Circumpolar Current, CDW is relatively warm (over 1 °C), saline and dense. In places, CDW approaches the Antarctic coast (Fig. 2) and is channelled at depth (typically deeper than ~300 m) along bathymetric troughs in the sea floor beneath the ice shelves[19]. At these depths, CDW is up to 4 °C above freezing and so can drive vigorous basal melt[10]. Many major Antarctic glaciers lie in retreated positions within glacially eroded troughs that span the continental shelf and deepen towards the ice sheet (Fig. 2), and so are well positioned to respond to CDW incursions.

Our observations support this explanation: the most rapid thinning occurs on thick ice shelves with relatively high sea-floor temperatures and deep bathymetric troughs spanning the continental shelf (Fig. 2). This is most apparent on the Amundsen Sea coast, where the only ice shelves not thinning (Abbott, Nickerson and Sulzberger) are those not exposed to deep-lying warm water because they have shallow drafts, lack deep bathymetric troughs or are remote from CDW (Figs 2 and 3). On the Antarctic Peninsula, thinning of the George VI Ice Shelf is also concentrated on the thickest area that is most likely to be exposed to shoaling CDW[7,20] (Figs 2 and 4).

Incursions of CDW can be driven by wind forcing, through upwelling along the continental shelf break[6,21] and vertical mixing. Mixing of CDW with colder, shallower layers over the continental shelf has been inferred following a wind-driven landward shift of the sea-ice formation zone[7]. The link between changing wind fields and heat redistribution in coastal Antarctica is poorly understood, but wind forcing has changed markedly over recent decades[22]. Increased circumpolar winds have caused strong warming of the Southern Ocean since the 1950s through a poleward shift in the Antarctic Circumpolar Current[23] and increased eddy heat flux[24]. Increased atmospheric flow over the Antarctic Peninsula since the 1960s has increased surface melt and initiated the collapse of the Larsen A and B ice shelves[8]. Changing cyclonic winds over the Amundsen Sea have brought a significant sea-ice decline and significant West Antarctic spring climate warming since the late 1970s[25]. These changes in wind forcing have been attributed to a combination of changing tropical Pacific sea surface temperatures[26,27], and stratospheric ozone loss and increased greenhouse

gases[28]. Less is known about CDW incursions and the role of wind forcing along the East Antarctic coast, where typically cooler waters bathe the continental shelf, but warm waters lie close offshore (Fig. 2).

To summarize, we find thinning attributed to ocean-driven basal melt on 20 of 54 ice shelves, with the most widespread and rapid losses (up to ~7 m yr^{-1}) on the coast of West Antarctica, where warm waters at depth have access to thick ice shelves via deep bathymetric troughs. There is evidence that changes in wind forcing explain both the increased oceanic supply of warm water to thinning West Antarctic ice shelves, and the atmospheric warming on the Antarctic Peninsula that caused the loss of Larsen A and B and now dominates the thinning of Larsen C. That is to say, both processes are ultimately linked to the atmosphere. Both mechanisms imply that Antarctic ice shelves can respond rapidly to Southern Hemisphere wind patterns that vary on timescales of years to decades.

We find that ocean-driven ice-shelf thinning is in all cases coupled with dynamic thinning of grounded tributary glaciers that together account for about 40% of Antarctic discharge and the majority of Antarctic ice-sheet mass loss[2]. In agreement with recent model predictions[17], we conclude that it is reduced buttressing from the thinning ice shelves that is driving glacier acceleration and dynamic thinning. This implies that the most profound contemporary changes to the ice sheets and their contribution to sea level rise can be attributed to ocean thermal forcing that is sustained over decades[12] and may already have triggered a period of unstable glacier retreat[9].

METHODS SUMMARY

Measuring change in ice-shelf thickness from altimetry is challenging because of confounding signals from tides, atmospheric pressure fluctuations, near-surface firn processes and sea-level rise. Furthermore, elevation change of the floating surface can represent anything from about 10% of total thickness change (for loss of relatively dense basal ice) to 100% (for loss of air trapped in near-surface firn). We use ICESat GLA12 Release-428 altimetry data from October 2003 to November 2008 (http://icesat.gsfc.nasa.gov/icesat) to measure height change[1]. We correct for confounding signals, subtracting the elevation change modelled for near-surface firn processes (surface mass balance and firn compaction). We use CATS2008A (http://www.esr.org/polar_tide_models/Model_CATS2008a.html) to model tides, RACMOv2.2/ANT27 to model climate and UUFIRNMODELv2.1/ANT to model firn height change (Supplementary Methods). Supplementary corrected ICESat and firn modelling data are available[29]. Where hydrostatic equilibrium applies, we calculate the underlying changes in ice thickness (ΔT) of the ice shelves from the corrected change in freeboard. Our error budget accounts for uncertainty in ICESat measurements, in the correction of each of the confounding signals and in our height change calculations. We find that the uncertainty in spatially averaged ICESat $\Delta h/\Delta t$ averages 0.007 m yr^{-1} but uncertainty in $\Delta T/\Delta t$ is dominated by uncertainties in the firn correction (averaging 0.09 m yr^{-1} and 0.02 m yr^{-1} respectively on ice shelves with and without melt) (Supplementary Methods).

We test for changes in volume due to changing glacier influx or ice-shelf geometry[4] using published measurements[2,13] and recent satellite images of ice-shelf extent (http://www.polarview.aq) (Supplementary Discussion). We then relate the pattern of our calculated ice shelf $\Delta T/\Delta t$ to bathymetry[30] (http://www.earth-syst-sci-data.net/2/261/2010/essd-2-261-2010.pdf) and sea-floor potential temperatures from the World Ocean Circulation Experiment Southern Ocean Atlas (http://woce.nodc.noaa.gov/wdiu/).

Received 6 October 2011; accepted 17 February 2012.

1. Pritchard, H. D., Arthern, R. J., Vaughan, D. G. & Edwards, L. A. Extensive dynamic thinning on the margins of the Greenland and Antarctic ice sheets. *Nature* **461,** 971–975 (2009).
2. Rignot, E. B. *et al.* Antarctic ice mass loss from radar interferometry and regional climate modelling. *Nature Geosci.* **1,** 106–110 (2008).
3. Solomon, S. *et al. Contribution of Working Group I to the Fourth Assessment Report of the Intergovernmental Panel on Climate Change* 2007 (Cambridge University Press, 2007).
4. Dupont, T. K. & Alley, R. B. Assessment of the importance of ice-shelf buttressing to ice-sheet flow. *Geophys. Res. Lett.* **32** (2005).
5. Rott, H., Rack, W., Skvarca, P. & de Angelis, H. Northern Larsen Ice Shelf, Antarctica: further retreat after collapse. *Ann. Glaciol.* **34,** 277–282 (2002).
6. Thoma, M., Jenkins, A., Holland, D. & Jacobs, S. Modelling Circumpolar Deep Water intrusions on the Amundsen Sea continental shelf, Antarctica. *Geophys. Res. Lett.* **35,** L18602 (2008).
7. Holland, P. R., Jenkins, A. & Holland, D. M. Ice and ocean processes in the Bellingshausen Sea, Antarctica. *J. Geophys. Res.* **115,** C05020 (2010).
8. Marshall, G. J., Orr, A., van Lipzig, N. P. M. & King, J. C. The impact of a changing Southern Hemisphere Annular Mode on Antarctic Peninsula summer temperatures. *J. Clim.* **19,** 5388–5404 (2006).
9. Schoof, C. Ice sheet grounding line dynamics: steady states, stability and hysteresis. *J. Geophys. Res.* **112,** F03S28 (2007).
10. Jacobs, S. S., Jenkins, A., Giulivi, C. F. & Dutrieux, P. Stronger ocean circulation and increased melting under Pine Island Glacier ice shelf. *Nature Geosci.* **4,** 519–523 (2011).
11. Rignot, E. & Jacobs, S. S. Rapid bottom melting widespread near Antarctic Ice Sheet grounding lines. *Science* **296,** 2020–2023 (2002).
12. Joughin, I., Smith, B. E. & Holland, D. M. Sensitivity of 21st century sea level to ocean-induced thinning of Pine Island Glacier, Antarctica. *Geophys. Res. Lett.* **37,** L20502 (2010).
13. Shepherd, A. W., Wallis, D., Giles, D., Laxon, K. & Sundal, S. A. V. Recent loss of floating ice and the consequent sea level contribution. *Geophys. Res. Lett.* **37,** L13503 (2010).
14. Shuman, C. A. *et al.* ICESat Antarctic elevation data: preliminary precision and accuracy assessment. *Geophys. Res. Lett.* **33,** L07501 (2006).
15. Holland, P. R. *et al.* The air content of Larsen Ice Shelf. *Geophys. Res. Lett.* **38,** L10503 (2011).
16. Tedesco, M. Assessment and development of snowmelt retrieval algorithms over Antarctica from K-band spaceborne brightness temperature (1979–2008). *Remote Sens. Environ.* **113,** 979–997 (2009).
17. Gagliardini, O., Durand, G., Zwinger, T., Hindmarsh, R. C. A. & Le Meur, E. Coupling of ice-shelf melting and buttressing is a key process in ice-sheets dynamics. *Geophys. Res. Lett.* **37,** L14501 (2010).
18. Murray, T. *et al.* Ocean regulation hypothesis for glacier dynamics in southeast Greenland and implications for ice sheet mass changes. *J. Geophys. Res.* **115,** F03026 (2010).
19. Wåhlin, A. K., Yuan, X., Bjork, G. & Nohr, C. Inflow of Warm Circumpolar Deep Water in the Central Amundsen Shelf. *J. Phys. Oceanogr.* **40,** 1427–1434 (2010).
20. Jenkins, A. & Jacobs, S. Circulation and melting beneath George VI Ice Shelf, Antarctica. *J. Geophys. Res.* **113,** C04013 (2008).
21. Martinson, D. G., Stammerjohn, S. E., Iannuzzi, R. A., Smith, R. C. & Vernet, M. Western Antarctic Peninsula physical oceanography and spatio-temporal variability. *Deep Sea Res. II* **55,** 1964–1987 (2008).
22. Young, I. R., Zieger, S. & Babanin, A. V. Global trends in wind speed and wave height. *Science* **332,** 451–455 (2011).
23. Gille, S. T. Decadal-scale temperature trends in the Southern Hemisphere Ocean. *J. Clim.* **21,** 4749–4765 (2008).
24. Hogg, A. M. C., Meredith, M. P., Blundell, J. R. & Wilson, C. Eddy heat flux in the Southern Ocean: response to variable wind forcing. *J. Clim.* **21,** 608–620 (2008).
25. Schneider, D., Deser, C. & Okumura, Y. An assessment and interpretation of the observed warming of West Antarctica in the austral spring. *Clim. Dyn.* **38** (1–2), 323–347 (2011).
26. Meredith, M. P. *et al.* Changes in the freshwater composition of the upper ocean west of the Antarctic Peninsula during the first decade of the 21st century. *Prog. Oceanogr.* **87,** 127–143 (2010).
27. Steig, E. J. Ding, Q. Battisti, D. S. & Jenkins, A. Tropical forcing of Circumpolar Deep Water Inflow and outlet glacier thinning in the Amundsen Sea Embayment, West Antarctica. *Ann. Glaciol.* **53,** 19–28 (2012).
28. Fyfe, J. C. & Saenko, O. A. Human-induced change in the Antarctic Circumpolar Current. *J. Clim.* **18,** 3068–3073 (2005).
29. Pritchard, H. D. *et al.* Corrected ICESat altimetry data, surface mass balance, and firn elevation change on Antarctic ice shelves. http://dx.doi.org/10.1594/PANGAEA.775984 (PANGAEA Data Publisher for Earth & Environmental Science, 2012).
30. Timmermann, R. *et al.* A consistent dataset of Antarctic ice sheet topography, cavity geometry, and global bathymetry. *Earth Syst. Sci. Data Discuss.* **3,** 231–257 (2010).
31. Bindschadler, R. C. *et al.* Getting around Antarctica: new high-resolution mappings of the grounded and freely-floating boundaries of the Antarctic ice sheet created for the International Polar Year. *The Cryosphere* **5,** 569–588 (2011).

Supplementary Information is linked to the online version of the paper at www.nature.com/nature.

Acknowledgements This work was supported by funding from the ice2sea programme from the European Union 7th Framework Programme, grant number 226375. This is ice2sea contribution number 056. We thank NASA's ICESat Science Project for distribution of the ICESat data (see http://icesat.gsfc.nasa.gov and http://nsidc.org/data/icesat). We also thank T. Urban for providing ICESat bias corrections and R. Arthern for assistance with error assessment. This paper is ESR contribution 146.

Author Contributions H.D.P. designed and led the research. H.D.P., H.A.F. and L.P. analysed the altimetry data. S.R.M.L. and M.R.v.d.B. modelled the firn signals. All authors wrote and discussed the paper.

Author Information Reprints and permissions information is available at www.nature.com/reprints. The authors declare no competing financial interests. Readers are welcome to comment on the online version of this article at www.nature.com/nature. Correspondence and requests for materials should be addressed to H.D.P. (h.pritchard@bas.ac.uk).